

# Bio-Inspired Stable $\{Co_4O_4\}$ Molecular Catalyst for the Oxygen Evolution Reaction

Shangkun Li<sup>§\*</sup> and Greta R. Patzke\*

<sup>§</sup>SCS-dsm-firmenich Award for Best Poster Presentation in Catalysis Sciences & Engineering

**Abstract:** Developing stable and efficient molecular water oxidation catalysts is crucial for renewable energy conversion. Cubic  $\{Co_4O_4\}$  complexes are promising oxygen-evolution-reaction (OER) catalysts because they combine molecular precision with bio-inspired design, but their operational stability remains a challenge. Inspired by the oxygen-evolving complex of photosystem II, we immobilize  $\{Co_4O_4\}$  cubane oxo clusters within a conductive polymer. Using polypyrrole as a p-type conducting polymer enhances hole transport during OER, resulting in a higher turnover frequency than the pristine  $\{Co_4O_4\}$  cluster and cobalt oxide benchmarks. The asymmetric coordination further improves stability and catalytic efficiency by exposing an active cofacial dihydroxide motif.<sup>[1]</sup>

**Keywords:** Conductive polymers · Molecular catalysts · Polynuclear clusters · Water splitting



**Shangkun Li** obtained his Bachelor's and Master's degrees in chemistry at Jilin University, followed by a PhD in chemistry at ETH Zurich, where he worked on the synthesis of photoluminescent nanocrystals in microfluidic systems under the supervision of Prof. Andrew deMello. In 2022, he joined Prof. Greta R. Patzke's group at the University of Zurich as a postdoctoral researcher. His research involves the design

of molecular catalysts and the study of early-stage assembly mechanisms in complex metal-organic structures through *in situ* optical detection integrated with microfluidic platforms.

## 1. Introduction

The development of efficient and durable water oxidation catalysts based on polynuclear metal-oxo clusters remains a significant challenge and opportunity in the context of converting renewable energy into chemical fuels.<sup>[2–6]</sup> Among these, cuboidal  $\{Co_4O_4\}$  clusters have garnered considerable attention as molecular water-oxidation catalysts, owing to their unique combination of heterogeneous and homogeneous catalytic properties, as well as their structural resemblance to biological systems.<sup>[7–10]</sup> However, their practical application in the oxygen-evolution reaction (OER) is limited by stability concerns, necessitating the development of effective stabilization strategies.

### 1.1 Asymmetrically Coordinated Cubanes

Proteins found in natural enzymatic systems, such as in photosystem II (PSII), set a good example for addressing aggregation issues as they offer tailored coordination environments for active sites and facilitate stable catalytic centres, such as for the OER (Fig. 1a).<sup>[11–15]</sup> The intricately organized and ligand-diverse coordination environment of PSII enables the  $\{CaMn_4O_5\}$  cluster to retain an asymmetrical structure, leading to the metal centres exhibiting distinct functionalities.<sup>[15]</sup> With this knowledge at hand, we set out to create a system (Fig. 1b) that features an asymmetric

cubane active site that is designed to prevent aggregation of the catalyst and that can also be further embedded in conductive matrices to enhance the OER activity.<sup>[16–18]</sup>

### 1.2 Conducting Substrate

Polypyrrole (Ppy) is a well-established conducting polymer, valued for its high conductivity, low toxicity, low cost, and straightforward synthesis.<sup>[19,20]</sup> Its tuneable organic framework allows for structural modification, creating suitable anchoring sites for  $\{Co_4O_4\}$  molecular catalysts.<sup>[21–23]</sup> Beyond providing structural stabilization, polypyrrole functions as a p-type conducting polymer, facilitating hole transport during the OER compared to both unmodified  $\{Co_4O_4\}$  clusters and conventional heterogeneous cobalt oxide catalysts.<sup>[24–27]</sup>

## 2. Structural Tailoring and Catalytic Performance

$Co_4O_4(OAc)_4(py)_4$  cubane ( $Co_4O_4-0$ ) was prepared and purified *via* column chromatography in accordance with established literature methods.<sup>[28,29]</sup> X-ray crystallographic analysis (Fig. 2a) confirmed the formation of  $Co_4O_4-0$  with a symmetric core stabilized by four acetate and four pyridine ligands, a structure that was further verified by <sup>1</sup>H NMR spectroscopy (Fig. 2b). For immobilization of  $\{Co_4O_4\}$  within the polypyrrole matrix, <sup>1</sup>H-pyrrole-1-propionic acid (ppa) was selected as the ligand. The unsaturated pyrrole ring of ppa enables polymerization into polypyrrole to form a conjugated network, while its carboxyl group can substitute the labile acetate ligands of the cubane complex.

### 2.1 Ligand Exchange on $\{Co_4O_4\}$ Cubane

The starting cubane,  $Co_4O_4-0$ , underwent a thermodynamically driven ligand-exchange process in which one acetate ligand was displaced by ppa (Fig. 2a).<sup>[30]</sup> Under stoichiometric control of ppa,  $Co_4O_4(OAc)_3(ppa)(py)_4$  ( $Co_4O_4-ppa_1$ ) was subsequently synthesized and purified by column chromatography. The successful formation of  $Co_4O_4-ppa_1$  was confirmed by <sup>1</sup>H NMR spectroscopy (Fig. 2b).

In the spectrum of  $Co_4O_4-ppa_1$ , the resonance at  $\delta=2.11$  ppm was assigned to the methyl protons ( $CH_3-COO$ ) of the acetate ligands. Pyridine-ring protons appeared as three sets of signals at 8.40–8.43 ppm, 7.64–7.70 ppm, and 7.17–7.21 ppm. Coordination of ppa was evidenced by characteristic proton signals at 6.61–6.68 ppm, 6.05–6.11 ppm, 4.05–4.28 ppm, and 2.66–2.87 ppm. Integration

\*Correspondence: Dr. S. Li, E-mail: shangkun.li@chem.uzh.ch;  
Prof. G. R. Patzke, E-mail: greta.patzke@chem.uzh.ch  
Department of Chemistry, University of Zurich, CH-8057 Zurich

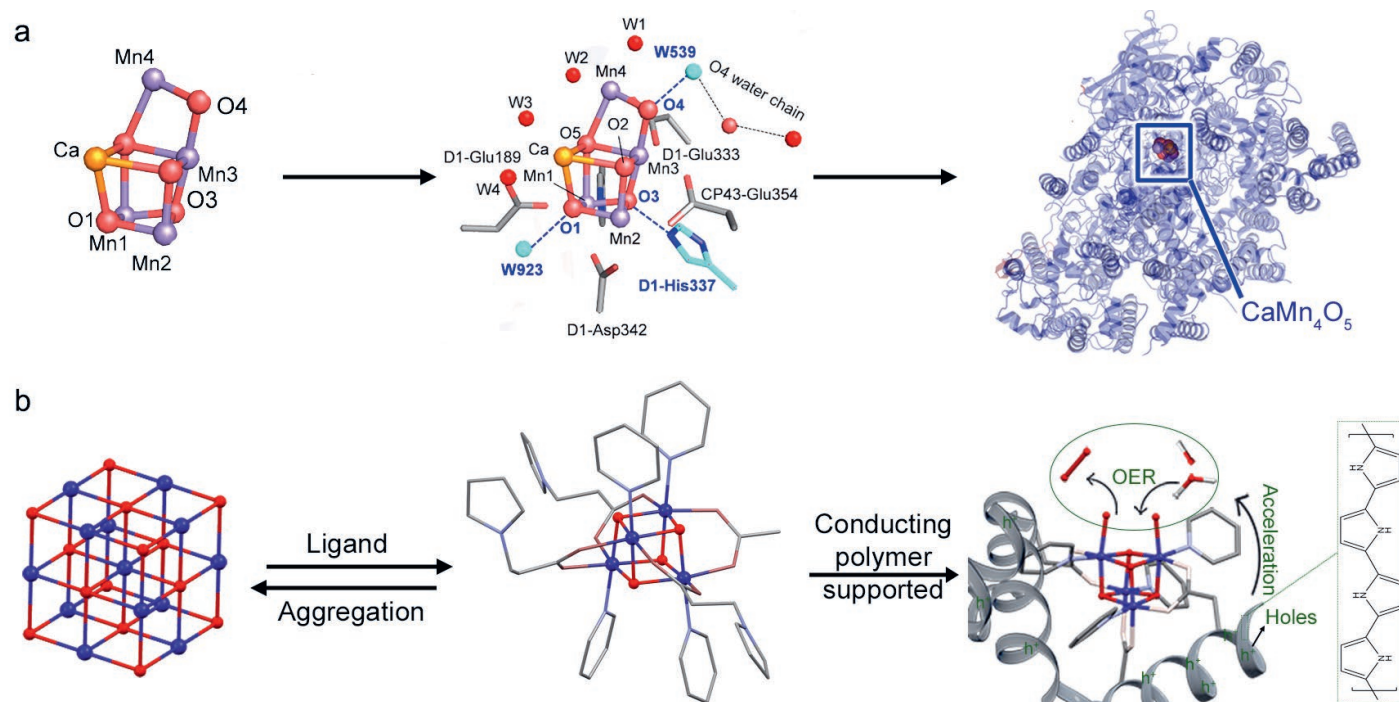


Fig. 1. Design of polypyrrole supported, asymmetric-coordinated cubanes inspired by PSII. (a) {CaMn<sub>4</sub>O<sub>5</sub>} OEC of PSII. (b) Bio-inspired stabilization of {Co<sub>4</sub>O<sub>4</sub>}; stabilized by asymmetric coordinated ligands, followed by a Ppy polymer as a second support layer. Part (a) was adapted from data in Ref. [11].

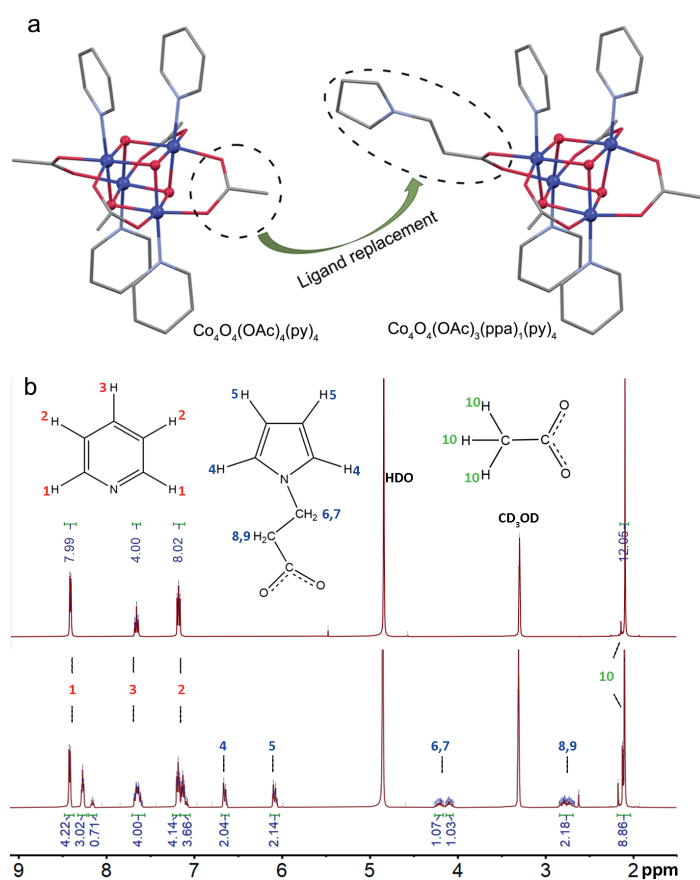


Fig. 2. Formation of asymmetrically coordinated cubane Co<sub>4</sub>O<sub>4</sub>-ppa<sub>1</sub> by ligand exchange and its electrochemical comparison with Co<sub>4</sub>O<sub>4</sub>-0. (a) Structural comparison of Co<sub>4</sub>O<sub>4</sub>-0 and Co<sub>4</sub>O<sub>4</sub>-ppa<sub>1</sub> (red, blue, gray, and light blue represent O, Co, C, and N, respectively). (b) <sup>1</sup>H NMR spectra of Co<sub>4</sub>O<sub>4</sub>-0 and Co<sub>4</sub>O<sub>4</sub>-ppa<sub>1</sub> in CD<sub>3</sub>OD. Adapted from Ref. [1] S. Li *et al.*, 2024, *Nature Communications*, 15. CC BY 4.0. Adapted with permission.

of these resonances gave a ppa/acetate/pyridine ratio of 1.02 : 2.95 : 4.00, in good agreement with the theoretical stoichiometry of Co<sub>4</sub>O<sub>4</sub>-ppa<sub>1</sub>. Beyond the mono-ppa-substituted complex Co<sub>4</sub>O<sub>4</sub>-ppa<sub>1</sub>, a series of higher-substituted cubanes Co<sub>4</sub>O<sub>4</sub>-ppa<sub>2</sub>, Co<sub>4</sub>O<sub>4</sub>-ppa<sub>3</sub>, and Co<sub>4</sub>O<sub>4</sub>-ppa<sub>4</sub> were also synthesized by reacting Co<sub>4</sub>O<sub>4</sub>-0 with progressively larger amounts of ppa. In this way, varying degrees of ligand exchange on the {Co<sub>4</sub>O<sub>4</sub>} cubane were systematically achieved through controlled ppa addition and subsequent purification.

Incorporation of a ppa ligand into the cubane framework disrupts the original symmetry, yielding an asymmetrically coordinated structure. Owing to the inert and relatively hydrophobic nature of the ppa ligand, the two Co centres bound to ppa are less susceptible to nucleophilic attack, making ligand substitution by hydroxide less favourable. As a result, formation of the cofacial dihydroxide intermediate from the asymmetrically coordinated Co<sub>4</sub>O<sub>4</sub>-ppa<sub>1</sub> becomes more favourable.<sup>[31]</sup>

Although this asymmetry reduces the likelihood of aggregation by decreasing the probability of matched orientations between cubane units, aggregation cannot be completely suppressed. Additional stabilization strategies are therefore required for the {Co<sub>4</sub>O<sub>4</sub>} cubane.

## 2.2 Immobilization through copolymerization

In natural PSII, the {CaMn<sub>4</sub>O<sub>5</sub>} inorganic core is embedded within a macromolecular protein scaffold that provides a precisely tailored catalytic environment. This biological paradigm motivates the use of polymer matrices to prevent aggregation of {Co<sub>4</sub>O<sub>4</sub>} units during water splitting. Among the Co<sub>4</sub>O<sub>4</sub>-ppa<sub>x</sub> series, Co<sub>4</sub>O<sub>4</sub>-ppa<sub>3</sub> was chosen based on two considerations: its asymmetric coordination environment and its higher ppa-to-cubane ratio. For preparation of the polymeric material, Co<sub>4</sub>O<sub>4</sub>-ppa<sub>3</sub> was oxidized with ceric ammonium nitrate in the presence of NH<sub>4</sub>PF<sub>6</sub> to yield [Co<sub>4</sub>O<sub>4</sub>-ppa<sub>3</sub>][PF<sub>6</sub>],<sup>[29]</sup> which served as both oxidizing agent and monomer to form Co<sub>4</sub>O<sub>4</sub>-ppa<sub>3</sub>-Ppy. The Ppy and ppa ligands were linked by covalent bonding (Fig. 3a–d). During the copolymerization process, Na<sub>2</sub>S<sub>2</sub>O<sub>8</sub> was used as an additional

oxidizing agent, while the  $\text{SO}_4^{2-}$  ions produced in the reaction acted as dopants in the conducting polymer.

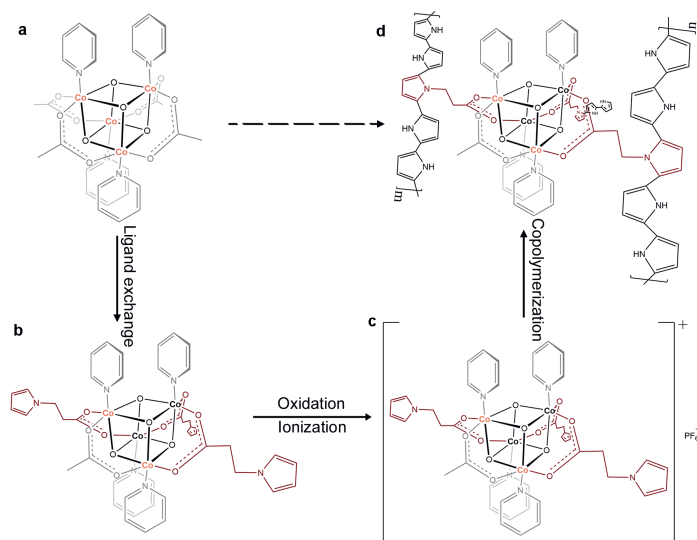


Fig. 3. Synthetic strategy of polymer-hybrid  $\{\text{Co}_4\text{O}_4\}$  cubane catalysts starting from  $\text{Co}_4\text{O}_4\text{-0}$ . Adapted from Ref. [1] S. Li *et al.*, **2024**, *Nature Communications*, **15**. CC BY 4.0. Adapted with permission.

### 2.3 Catalytic Performance of Embedded $\{\text{Co}_4\text{O}_4\}$

The OER performances of  $\text{Co}_4\text{O}_4\text{-0}$ ,  $\text{Co}_4\text{O}_4\text{-ppa}_3$ ,  $\text{Co}_4\text{O}_4\text{-ppa}_3\text{-Ppy}$ , and  $\text{Ppy-ppa}$  were investigated in 1.0 M KOH using a standard three-electrode setup and compared with  $\text{CoOOH}$  and  $\text{Co}_3\text{O}_4$  as benchmarks. Linear sweep voltammetry (LSV) curves were collected without  $iR$  (ohmic) compensation (Fig. 4a).  $\text{Co}_4\text{O}_4\text{-0}$  exhibited an onset potential of  $\sim 1.62$  V vs the reversible hydrogen electrode (RHE). Upon substitution of three acetate ligands with ppa,  $\text{Co}_4\text{O}_4\text{-ppa}_3$  showed improved catalytic activity, with the onset potential decreasing to  $\sim 1.57$  V vs RHE. This enhancement

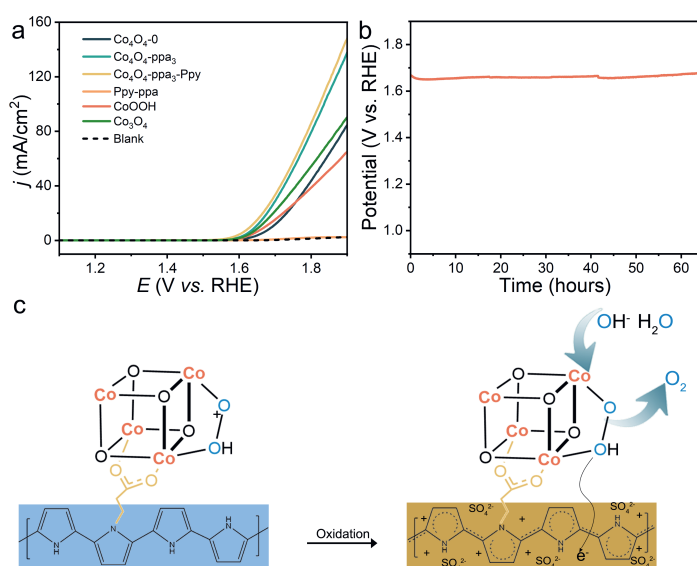


Fig. 4. OER catalytic performance of  $\text{Co}_4\text{O}_4\text{-0}$ ,  $\text{Co}_4\text{O}_4\text{-ppa}_3$ ,  $\text{Co}_4\text{O}_4\text{-ppa}_3\text{-Ppy}$ ,  $\text{Ppy-ppa}$ ,  $\text{CoOOH}$ , and  $\text{Co}_3\text{O}_4$ , and proposed role of  $\text{SO}_4^{2-}$ -doped Ppy during catalysis. (a) Linear sweep voltammograms of OER for  $\text{Co}_4\text{O}_4\text{-0}$ ,  $\text{Co}_4\text{O}_4\text{-ppa}_3$ ,  $\text{Co}_4\text{O}_4\text{-ppa}_3\text{-Ppy}$ ,  $\text{Ppy-ppa}$ ,  $\text{CoOOH}$ , and  $\text{Co}_3\text{O}_4$  at a scan rate of  $10$   $\text{mV s}^{-1}$  in 1 M KOH. (b) OER stability test of  $\text{Co}_4\text{O}_4\text{-ppa}_3\text{-Ppy}$  at  $20$   $\text{mA cm}^{-2}$ . (c) Proposed function of p-type Ppy during OER. Adapted from Ref. [1] S. Li *et al.*, **2024**, *Nature Communications*, **15**. CC BY 4.0. Adapted with permission.

indicates that incorporation of the inert ppa ligands does not impede OER catalysis, but instead favourably modulates the activity of the cubane.

Copolymerization of  $\text{Co}_4\text{O}_4\text{-ppa}_3$  with polypyrrole produced  $\text{Co}_4\text{O}_4\text{-ppa}_3\text{-Ppy}$ , which exhibited the highest OER activity among all the tested samples, with an onset potential of  $\sim 1.55$  V vs RHE. In contrast, both benchmark catalysts displayed onset potentials of  $\sim 1.59$  V vs RHE. Control experiments using the pristine  $\text{SO}_4^{2-}$ -doped Ppy-ppa copolymer (Fig. 4a) showed negligible OER activity relative to the blank electrode, confirming that the polymer matrix itself is not catalytically active. The superior performance of  $\text{Co}_4\text{O}_4\text{-ppa}_3\text{-Ppy}$  therefore originates from the immobilized cubane units, indicating that isolated cubane sites within the Ppy framework promote faster kinetics and higher intrinsic activity.<sup>[32]</sup> The operational stability of  $\text{Co}_4\text{O}_4\text{-ppa}_3\text{-Ppy}$  was evaluated by chronopotentiometry at a constant current density of  $20$   $\text{mA cm}^{-2}$  for more than 60 h (Fig. 4b). The catalyst maintained stable performance with minimal potential change over time, demonstrating excellent durability under OER conditions.

Overall, polypyrrole plays a crucial role in both enhancing catalytic activity, by facilitating electron withdrawal from key cubane intermediates (Fig. 4c) and stabilizing the  $\{\text{Co}_4\text{O}_4\}$  active centres, enabling efficient and sustained OER performance.

### 3. Conclusions

Through combining ligand substitution with a polymer-hybrid strategy, a highly active and stable molecular catalyst is designed for OER. Firstly, a symmetric  $\text{Co}_4\text{O}_4\text{-0}$  cubane was modified by ligand exchange to generate asymmetrically coordinated  $\text{Co}_4\text{O}_4\text{-ppa}_1$ .  $\text{Co}_4\text{O}_4\text{-ppa}_1$  showed better stability compared with  $\text{Co}_4\text{O}_4\text{-0}$  under OER conditions. In light of the enhanced performance of  $\text{Co}_4\text{O}_4\text{-ppa}_1$ , a further substituted  $\{\text{Co}_4\text{O}_4\}$  cubane with three ppa ligands and one acetate ligand,  $\text{Co}_4\text{O}_4\text{-ppa}_3$ , was then synthesized. The  $\text{Co}_4\text{O}_4\text{-ppa}_3$  cubane retained the advantages of the asymmetric structure. Embedded  $\text{Co}_4\text{O}_4\text{-ppa}_3$  cubanes in the p-type conducting polymer Ppy facilitated efficient electron transfer and afforded sustained catalytic activity during OER.

### Acknowledgements

The authors thank the Swiss Chemical Society and dsm-firmenich for the best poster award. We are grateful to the University of Zurich and to the Swiss National Science Foundation Grant No. (200021\_200989/1) for financial support.

Received: January 22, 2026

- [1] S. Li, Z. Zhang, W. R. Marks, X. Huang, H. Chen, D. C. Stoian, R. Erni, C. A. Triana, G. R. Patzke, *Nat. Commun.* **2024**, *15*, 8432, <https://doi.org/10.1038/s41467-024-52514-z>.
- [2] A. K. Mengele, S. Rau, *JACS Au* **2023**, *3*, 36, <https://doi.org/10.1021/jacsau.2c00507>.
- [3] A. I. Nguyen, K. M. Van Allsburg, M. W. Terban, M. Bajdich, J. Oktawiec, J. Amtawong, M. S. Ziegler, J. P. Dombrowski, K. V. Lakshmi, W. S. Drisdell, J. Yano, S. J. L. Billinge, T. D. Tilley, *Proc. Natl. Acad. Sci. U. S. A.* **2019**, *116*, 11630, <https://doi.org/10.1073/pnas.1815013116>.
- [4] C. Zhang, C. Chen, H. Dong, J.-R. Shen, H. Dau, J. Zhao, *Science* **2015**, *348*, 690, <https://doi.org/10.1126/science.aaa6550>.
- [5] B. Schwarz, J. Forster, M. K. Goetz, D. Yücel, C. Berger, T. Jacob, C. Streb, *Angew. Chem. Int. Ed.* **2016**, *55*, 6329, <https://doi.org/10.1002/anie.201601799>.
- [6] J. Lin, X. Meng, M. Zheng, B. Ma, Y. Ding, *Appl. Catal. B Environ.* **2019**, *241*, 351, <https://doi.org/10.1016/j.apcatb.2018.09.052>.
- [7] J. Amtawong, A. I. Nguyen, T. D. Tilley, *J. Am. Chem. Soc.* **2022**, *144*, 1475, <https://doi.org/10.1021/jacs.1c11445>.
- [8] F. Evangelisti, R. Güttinger, R. Moré, S. Lubner, G. R. Patzke, *J. Am. Chem. Soc.* **2013**, *135*, 18734, <https://doi.org/10.1021/ja4098302>.
- [9] F. Song, K. Al-Ameed, M. Schilling, T. Fox, S. Lubner, G. R. Patzke, *J. Am. Chem. Soc.* **2019**, *141*, 8846, <https://doi.org/10.1021/jacs.9b01356>.

- [10] F. Song, R. Moré, M. Schilling, G. Smolentsev, N. Azzaroli, T. Fox, S. Luber, G. R. Patzke, *J. Am. Chem. Soc.* **2017**, *139*, 14198, <https://doi.org/10.1021/jacs.7b07361>.
- [11] K. Saito, S. Nakao, H. Ishikita, *Front. Plant Sci.* **2023**, *14*, <https://doi.org/10.3389/fpls.2023.1029674>.
- [12] M. Suga, F. Akita, K. Hirata, G. Ueno, H. Murakami, Y. Nakajima, T. Shimizu, K. Yamashita, M. Yamamoto, H. Ago, J.-R. Shen, *Nature* **2015**, *517*, 99, <https://doi.org/10.1038/nature13991>.
- [13] J. Zabret, S. Bohn, S. K. Schuller, O. Arnolds, M. Möller, J. Meier-Credo, P. Liauw, A. Chan, E. Tajkhorshid, J. D. Langer, R. Stoll, A. Krieger-Liszkay, B. D. Engel, T. Rudack, J. M. Schuller, M. M. Nowaczyk, *Nat. Plants* **2021**, *7*, 524, <https://doi.org/10.1038/s41477-021-00895-0>.
- [14] K. Lenzen, M. Planchestainer, I. Feller, D. R. Padrosa, F. Paradisi, M. Albrecht, *Chem. Commun.* **2021**, *57*, 9068, <https://doi.org/10.1039/D1CC03158A>.
- [15] J. S. Kanady, P.-H. Lin, K. M. Carsch, R. J. Nielsen, M. K. Takase, W. A. I. Goddard, T. Agapie, *J. Am. Chem. Soc.* **2014**, *136*, 14373, <https://doi.org/10.1021/ja508160x>.
- [16] J.-H. Kruse, M. Langer, I. Romanenko, I. Trentin, D. Hernández-Castillo, L. González, F. H. Schacher, C. Streb, *Adv. Funct. Mater.* **2022**, *32*, 2208428, <https://doi.org/10.1002/adfm.202208428>.
- [17] C. Zhao, Z. Chen, R. Shi, X. Yang, T. Zhang, *Adv. Mater.* **2020**, *32*, 1907296, <https://doi.org/10.1002/adma.201907296>.
- [18] Z. Chen, S. Pronkin, T.-P. Feller, K. Kailasam, G. Vilé, D. Albani, F. Krumeich, R. Leary, J. Barnard, J. M. Thomas, J. Pérez-Ramírez, M. Antonietti, D. Dontsova, *ACS Nano* **2016**, *10*, 3166, <https://doi.org/10.1021/acsnano.5b04210>.
- [19] S. Li, X. Lu, X. Li, Y. Xue, C. Zhang, J. Lei, C. Wang, *J. Colloid Interface Sci.* **2012**, *378*, 30, <https://doi.org/10.1016/j.jcis.2012.03.065>.
- [20] Y. Shi, L. Peng, Y. Ding, Y. Zhao, G. Yu, *Chem. Soc. Rev.* **2015**, *44*, 6684, <https://doi.org/10.1039/C5CS00362H>.
- [21] Y. Gu, J. Wang, M. Pan, S. Li, G. Fang, S. Wang, *Sens. Actuators, B Chem.* **2019**, *283*, 571, <https://doi.org/10.1016/j.snb.2018.12.046>.
- [22] Z. Fang, P. Wu, K. Yu, Y. Li, Y. Zhu, P. J. Ferreira, Y. Liu, G. Yu, *ACS Nano* **2019**, *13*, 14368, <https://doi.org/10.1021/acsnano.9b07826>.
- [23] J. Y. Lee, C. E. Schmidt, *J. Biomed. Mater. Res., Part A* **2015**, *103*, 2126, <https://doi.org/10.1002/jbm.a.35344>.
- [24] B. Zhang, H. Liu, P. Zhai, R. Zhang, W. Wang, P. Khangale, D. Hildebrandt, X. Liu, S. Qiao, *Adv. Funct. Mater.* **2023**, *33*, 2211440, <https://doi.org/10.1002/adfm.202211440>.
- [25] J.-X. Feng, S.-Y. Tong, Y.-X. Tong, G.-R. Li, *J. Am. Chem. Soc.* **2018**, *140*, 5118, <https://doi.org/10.1021/jacs.7b12968>.
- [26] L. Xu, Y. Zhang, L. Feng, X. Li, Y. Cui, Q. An, *ACS Appl. Mater. Interfaces* **2021**, *13*, 734, <https://doi.org/10.1021/acsami.0c20176>.
- [27] W. Mahfoz, Md. Abdul Aziz, S. Shaheen Shah, A.-R. Al-Betar, *Chem. – Asian J.* **2020**, *15*, 4358, <https://doi.org/10.1002/asia.202001163>.
- [28] N. S. McCool, D. M. Robinson, J. E. Sheats, G. C. Dismukes, *J. Am. Chem. Soc.* **2011**, *133*, 11446, <https://doi.org/10.1021/ja203877y>.
- [29] A. I. Nguyen, M. S. Ziegler, P. Oña-Burgos, M. Sturzbecher-Hohne, W. Kim, D. E. Bellone, T. D. Tilley, *J. Am. Chem. Soc.* **2015**, *137*, 12865, <https://doi.org/10.1021/jacs.5b08396>.
- [30] A. I. Nguyen, J. Wang, D. S. Levine, M. S. Ziegler, T. D. Tilley, *Chem. Sci.* **2017**, *8*, 4274, <https://doi.org/10.1039/C7SC00627F>.
- [31] A. M. Ullman, C. N. Brodsky, N. Li, S.-L. Zheng, D. G. Nocera, *J. Am. Chem. Soc.* **2016**, *138*, 4229, <https://doi.org/10.1021/jacs.6b00762>.
- [32] R. Gonçalves, R. S. Paiva, A. M. R. Ramirez, J. A. Mwanda, E. C. Pereira, A. Cuesta, *Electrochem. Sci. Adv.* **2022**, *2*, e2100028, <https://doi.org/10.1002/elsa.202100028>.

#### License and Terms



This is an Open Access article under the terms of the Creative Commons Attribution License CC BY 4.0. The material may not be used for commercial purposes.

The license is subject to the CHIMIA terms and conditions: (<https://chimia.ch/chimia/about>).

The definitive version of this article is the electronic one that can be found at <https://doi.org/10.2533/chimia.2026.250>